Butterfly interconnection networks and their applications in information processing and optical computing: applications in fast-Fourier-transform-based optical information processing

De-Gui Sun, Na-Xin Wang, Li-Ming He, Zhen-Wu Lu, and Zhao-Heng Weng

As modern optical information processing has developed, research on massive and parallel rapid computing and processing has attracted more attention. In this paper, butterfly networks and a variety of types of optical information processing are studied and discussed. For a basis, one- and two-dimensional butterfly interconnection networks are studied in constructions, and the relationship and the transformation between them are provided. Algorithms for both the one- and two-dimensional fast Fourier transforms are analyzed, one- and two-dimensional butterfly networks for implementing the algorithms are built, and computer-simulation results are attained. Finally, an underlying optical network system is suggested and studied in respect to its architecture and advantages; it is a new optical butterfly network hardware system consisting of two-dimensional binary phase diffraction gratings, which perform a variety of types of fast-Fourier-transform-based optical information processing.

Key words: Optical butterfly interconnection, butterfly network, optical butterfly network hardware system, optical information processing.

1. Introduction

As early as 1964 VanderLugt's concept of coherent spatial filtering brought optical information processing into wide use. Since that time, a variety of optical information-processing theories and applications have stimulated further study. This vigorous trend has continued and greatly developed, not only because optical systems are capable of performing certain complex operations, but also because the underlying physical theory has been introduced in an input–output system model.[1,2] Especially, optical information processing that includes digital signal processing and analog image processing has recently been widely studied and developed.[3–6] The advantages of optical information processing have attracted more and more interest with new developments and applications of current optical science, such as optical pattern recognition, target tracking, radar signal processing, optical computing, and optical communication.[7–10] Furthermore, the trend of digitized and parallelized rapid optical information processing has shown promising development. As a result, the research on optical interconnections for implementing optical information processing shows high potential because optical interconnections have desirable characteristics such as massive capacity, parallelism, and transmission in free space, which are suitable for massive parallel rapid processing.[3–6,11,12]

Recently, researchers of optical information processing have derived some approximate equations for computing the functions of interconnections and have attained the possibility of implementing the equations. Flow diagrams are constructed for the algorithms in such a way as to exhibit maximum parallelism. The operations are represented as nodes and connections. The flow diagrams are applied to an optical interconnection system, and the nodes indicate available functional elements.[11,12] Optical

L. M. He is with the Department of Electronic Engineering, Jilin University of Technology, Changchun 130025, China. The other authors are with the State Key Laboratory of Applied Optics, Changchun Institute of Optics and Fine Mechanics, Academia Sinica, P.O. Box 1024, Changchun 130022, China.

Received 20 November 1991.
0003-6935/93/357184-10$06.00/0.

interconnections have some advantages over electronic interconnections, such as reduced effective capacity loading and increased immunity to mutual interference in connecting multiprocessors.[13,14] The developments of some new optical logic devices and technologies, such as spatial light modulators[7,9,15] and symmetric self-electro-optic-effect devices,[16] suggest that optical interconnections may become available. The cost, speed, and size of these connections will likely be greater than those for conventional semiconductor techniques.

The algorithms and architecture of optical information processing include spatial filtering, frequency-spectrum analysis, convolution, correlation, distinct-feature extraction, and edge enhancement. They are based on Fourier transformations and Walsh–Hadamard transformations, which are the basic optical information-processing algorithms.[2,17,18] Therefore the purpose of this paper is to study a synthetic optical butterfly network hardware (OBNH) system for the fast Fourier transforms (FFT's) to implement optical information processing, since the FFT's are based on the butterfly flow-diagram algorithms.

To make the optical interconnection network system easily understood, we first define and discuss the construction and characteristics of the one-dimensional (1-D) and two-dimensional (2-D) butterfly interconnection networks by using the mathematical expressions and matrices corresponding to 1-D and 2-D FFT's, respectively. Then in Section 2 we study the relationships between the 1-D and 2-D butterfly networks and the conversion from the 2-D butterfly network to the 1-D network. Next, in Section 3 we study and discuss the construction of flow diagrams of the FFT's. In Section 4 we propose and study a 2-D OBNH system for implementing the FFT's. In Section 5 we provide the architecture and pattern designs of the binary phase diffraction gratings (BPDG's) and masks used in the system. Finally in Section 6 we give our summary and conclusions.

2. One- and Two-Dimensional Butterfly Interconnection Networks

The 1-D butterfly network is the primary model for studying and discussing all butterfly networks. The topology of a multistage network is defined by three physical parameters: (1) the type of switching element comprising a node, (2) the number of node stages, and (3) the link interconnections provided between adjacent node stages.[19,20] Both fully connected butterfly networks with N nodes and fully connected data manipulator networks with N nodes require $\log_2^N + 1$ node stages, in which each node stage is labeled in sequence from 0 to $\log_2^N$. The input (leftmost) node stage is assigned label 0, and the output (rightmost) node stage is assigned label $\log_2^N$. Each switching element (node) in a particular node stage is assigned a unique physical address with an address bit $(K_{i-1}, K_{i-2}, \ldots, K_0)$, where $i = \log_2^N$. The physical address identifies the element's relative location within the node stage, with the top node labeled as 0 and the bottom node labeled as $N - 1$.[20,21]

In the 1-D butterfly networks a pair of interconnections provided by the links within link stage i can be mapped as B_i^0 and B_i^1. These points represent the straightforward connection and the butterfly connection, respectively,[21] and they map a node $(K_{i-1}, \ldots, K_i, \ldots, K_0)_i$ in node stage i two nodes in node stage $i + 1$. The relationships between the node in node stage i and the two nodes in node stage $i + 1$ are described by

$$B_i^0(K_{i-1}K_{i-2}, \ldots, K_i, \ldots, K_0) = (K_iK_{i-1}, \ldots, K_{1-i+1}, \ldots, 0, \ldots, K_{1-i-1}, \ldots, K_1)_{i+1} \quad \text{for link } (K_{i-1}K_{i-2}, \ldots, K_1)_{i+1}, \quad 0 \leqslant i < 1, \quad (1)$$

$$B_i^1(K_{i-1}K_{i-2}, \ldots, K_i, \ldots, K_0) = (K_iK_{i-1}, \ldots, K_{1-i+1}, \ldots, 1, \ldots, K_{1-i-1}, \ldots, K_1)_{i+1} \quad \text{for link } (K_{i-1}K_{i-2}, \ldots, K_1)_{i+1}, \quad 0 \leqslant i < 1. \quad (2)$$

Then for the $(i + 1)$th stage the link relationship of K_{i+1} is shown by

$$K_{i+1}^0 = K_i, \quad K_i = 0, 1, \ldots, N - 1, \quad 0 \leqslant i < 1, \quad (3)$$

$$K_{i+1}^1 = \begin{cases} K_i + N/2^i & [(j-1)N/2^i < K_{i+1}^1 \leqslant jN/2^i] \\ K_i - N/2^i & [jN/2^i \leqslant K_{i+1}^1 < jN/2^i] \end{cases} \quad (j = 1, 2, \ldots, 2^i). \quad (4)$$

In terms of the above butterfly network theorem, we can attain a butterfly network with $N = 8$ size and $l = 3$ link stages, as shown in Fig. 1.

As described in the introduction, almost all optical information processing is performed in 2-D parallel forms and requires 2-D optical interconnections; i.e., the images and/or signals to be processed are generally placed on 2-D planes. Figure 2 is a multistage 2-D butterfly interconnection network with $N \times N = 4 \times 4$ size. In the 2-D butterfly network the number of fan-in or fan-out lines on every node is four (rather than two). Thus a multistage 2-D butterfly interconnection network with $N \times N$ nodes has $n = \log_{2\times2}^{N\times N} = \log_2^N$, which corresponds to a 1-D network. In this

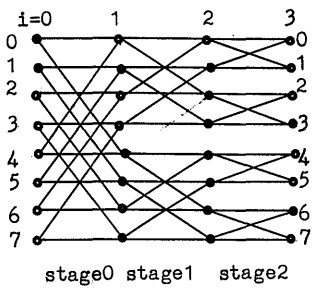

Fig. 1. 1-D butterfly network with $N = 8$.

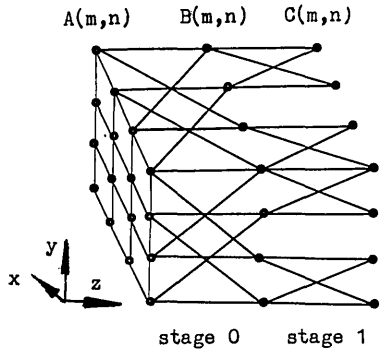

Fig. 2. 2-D butterfly network with $N \times N = 4 \times 4$.

paper we consider a 2-D butterfly interconnection network with 4 × 4 nodes, as shown in Fig. 2 (i.e., $n = \log_2^4 = 2$), and we represent the 2-D patterns of node distribution on planes A, B, and C as the matrix forms described in Table 1. Figure 2 and Table 1 are the mathematical definitions of the 2-D butterfly interconnection network. To make the corresponding relationship of the 2-D and 1-D butterfly interconnection networks clear, we derive the transformation pattern for changing the 2-D butterfly network into a the 1-D network, as shown in Fig. 3. It is easily noted that the 1-D network in Fig. 3 is composed of two stages of different 1-D interconnection networks, and each of the two stages has its own construction features, which are helpful for understanding and applying the 2-D butterfly interconnection networks. The 2-D butterfly networks and the transformations from 2-D to 1-D networks are different from the counterparts of crossover and perfect-shuffle networks in their construction and properties.[21,22] Therefore the above discussion about 1-D and 2-D butterfly interconnection network theory is a foundation for the following description about the applications of the butterfly interconnection networks.

Table 1. Elements from Matrix A to Matrix B to Matrix C of Fig. 2

Matrix A			
$A(0, 0)$	$A(0, 1)$	$A(0, 2)$	$A(0, 3)$
$A(1, 0)$	$A(1, 1)$	$A(1, 2)$	$A(1, 3)$
$A(2, 0)$	$A(2, 1)$	$A(2, 2)$	$A(2, 3)$
$A(3, 0)$	$A(3, 1)$	$A(3, 2)$	$A(3, 3)$
Matrix B			
$B(0, 0)$	$B(0, 1)$	$B(0, 2)$	$B(0, 3)$
$B(1, 0)$	$B(1, 1)$	$B(1, 2)$	$B(1, 3)$
$B(2, 0)$	$B(2, 1)$	$B(2, 2)$	$B(2, 3)$
$B(3, 0)$	$B(3, 1)$	$B(3, 2)$	$B(3, 3)$
Matrix C			
$C(0, 0)$	$C(0, 1)$	$C(0, 2)$	$C(0, 3)$
$C(1, 0)$	$C(1, 1)$	$C(1, 2)$	$C(1, 3)$
$C(2, 0)$	$C(2, 1)$	$C(2, 2)$	$C(2, 3)$
$C(3, 0)$	$C(3, 1)$	$C(3, 2)$	$C(3, 3)$

Table 2. Corresponding Relationships of Table 1

From Matrix A to Matrix B

$A(0, 0) \rightarrow B(0, 0), B(2, 0), B(0, 2), B(2, 2)$
$A(1, 0) \rightarrow B(1, 0), B(3, 0), B(1, 2), B(3, 2)$
$A(2, 0) \rightarrow B(2, 0), B(0, 0), B(2, 2), B(0, 2)$
$A(3, 0) \rightarrow B(3, 0), B(1, 0), B(3, 2), B(1, 2)$
$A(0, 1) \rightarrow B(0, 1), B(2, 1), B(0, 3), B(2, 3)$
$A(1, 1) \rightarrow B(1, 1), B(3, 1), B(1, 3), B(3, 3)$
$A(2, 1) \rightarrow B(2, 1), B(0, 1), B(2, 3), B(0, 3)$
$A(3, 1) \rightarrow B(3, 1), B(1, 1), B(3, 3), B(1, 3)$
$A(0, 2) \rightarrow B(0, 2), B(2, 2), B(0, 0), B(2, 0)$
$A(1, 2) \rightarrow B(1, 2), B(3, 2), B(1, 0), B(3, 0)$
$A(2, 2) \rightarrow B(2, 2), B(0, 2), B(2, 0), B(0, 0)$
$A(3, 2) \rightarrow B(3, 2), B(1, 2), B(3, 0), B(1, 0)$
$A(0, 3) \rightarrow B(0, 3), B(2, 3), B(0, 1), B(2, 1)$
$A(1, 3) \rightarrow B(1, 3), B(3, 3), B(1, 1), B(3, 1)$
$A(2, 3) \rightarrow B(2, 3), B(0, 3), B(2, 1), B(0, 1)$
$A(3, 3) \rightarrow B(3, 3), B(1, 3), B(3, 1), B(1, 1)$

From Matrix B to Matrix C

$B(0, 0) \rightarrow C(0, 0), C(1, 0), C(0, 1), C(1, 1)$
$B(1, 0) \rightarrow C(1, 0), C(0, 0), C(1, 1), C(0, 1)$
$B(2, 0) \rightarrow C(2, 0), C(3, 0), C(2, 1), C(3, 1)$
$B(3, 1) \rightarrow C(3, 0), C(2, 0), C(3, 1), C(2, 1)$
$B(0, 1) \rightarrow C(0, 1), C(1, 1), C(0, 0), C(1, 0)$
$B(1, 1) \rightarrow C(1, 1), C(0, 1), C(1, 0), C(0, 0)$
$B(2, 1) \rightarrow C(2, 1), C(3, 1), C(2, 0), C(3, 0)$
$B(3, 1) \rightarrow C(3, 1), C(2, 1), C(3, 0), C(2, 0)$
$B(0, 2) \rightarrow C(0, 2), C(1, 2), C(0, 3), C(1, 3)$
$B(1, 2) \rightarrow C(1, 2), C(0, 2), C(1, 3), C(0, 3)$
$B(2, 2) \rightarrow C(2, 2), C(3, 2), C(2, 3), C(3, 3)$
$B(3, 2) \rightarrow C(3, 2), C(2, 2), C(3, 3), C(2, 3)$
$B(0, 3) \rightarrow C(0, 3), C(1, 3), C(0, 2), C(1, 2)$
$B(1, 3) \rightarrow C(1, 3), C(0, 3), C(1, 2), C(0, 2)$
$B(2, 3) \rightarrow C(2, 3), C(3, 3), C(2, 2), C(3, 2)$
$B(3, 3) \rightarrow C(3, 3), C(2, 3), C(3, 2), C(2, 2)$

3. Butterfly Interconnection Networks in Fast Fourier Transforms

As we have shown, optical information processing includes spectral analysis, spatial and spectral filtering,[2,17] convolution and correlation,[2–5] feature extraction, edge enhancement, and pattern recognition. There are two major types of optical information-processing systems that depend on the light sources. One is incoherent light processing, and the other is coherent light processing. Figure 4 is a common optical information-processing system that is suitable for both coherent and incoherent sources. In coherent sources, input signals are illuminated by coherent light. This optical information-processing system is a 4-f configuration, where P_1 is the input plane, P_2 is the spectrum plane, and P_3 is the output plane. With the input signal function in P_1 as $f(x, y)$, the reference, or filtering, signal function as $h(x, y)$, the spectrum function in P_2 as $P(u, v)$, and the output signal function as $g(x', y')$, there are some optical transformation relations corresponding to various types of optical information processing. For spectrum analysis, only the first half of the system

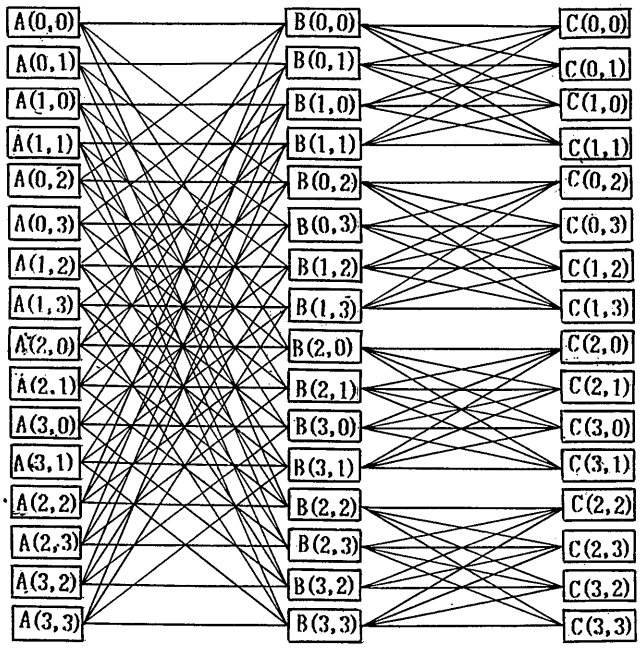

Fig. 3. Transform pattern for changing the 2-D butterfly network shown in Fig. 2 into a 1-D network.

(between P_1 and P_2) in Fig. 4 is required, and the relation is given as[2,22]

$$P(u, v) = F[f(x, y)]. \tag{5}$$

A spectrum detector is required at P_2. For recognition systems based on both matched filtering and correlation, the spectrum distribution $P(u, v)$ in plane P_2 is the product of Fourier transformation of the processed signal (or image) $F(u, v) = F[f(x, y)]$ with the conjugate of the Fourier transformation of the reference signal (or image) $H(u, v) = F[h(x, y)]$, which can be expressed as[1–6,16]

$$P(u, v) = F(u, v)H(u, v)^* \tag{6}$$

Then at output plane P_3, output function $g(x', y')$ is the inverse Fourier transformation of spectrum function $P(u, v)$:

$$g(x', y') = F^{-1}[P(u, v)]. \tag{7}$$

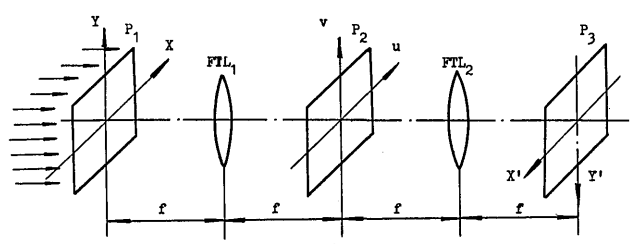

Fig. 4. General optical information-processing system: P_1, input plane; P_2, spectrum plane; P_3, output plane; FTL_1, FTL_2, two Fourier-transform lenses; f's, focal lengths.

It is necessary to explain that for both the matched-filtering method and the correlation (or joint-transformation correlation) method, there are two approaches of adding the reference function $h(x, y)$ or its Fourier transformation spectrum $H(u, v)$.[1–6] The first method is frequency-domain synthesis, in which a complex coherent optical information-processing spatial filter of the frequency spectrum is introduced in the frequency domain at plane P_2, and the filtering for the correlating operation is performed directly on the frequency-plane. Second is spectral-domain synthesis, in which a complex or real reference function is introduced in the input spatial domain, and the filtering, or correlation, operation is directly performed on the processing signal, or input plane. Therefore a general optical information-processing system is a one-stage Fourier transformation, as described in Eqs. (5) and (6), and also one-stage inverse Fourier transformations, as described in Eq. (7). Thus the research on the FFT algorithms in optical information processing has advanced greatly.[1,10]

We first consider the discrete Fourier transformation of a 1-D series

$$X(m) = \sum_{n=0}^{N-1} X(n)\exp(-j2\pi mn/N). \tag{8}$$

Let $W = \exp(-j2\pi/N)$; we separate the series $X(n)$ into two parts:

$$\begin{aligned} X_1(n) &= X(n), && n = 0, 1, \ldots, N/2 - 1, \\ X_2(n) &= X(n + N/2), && n = 0, 1, \ldots, N/2 - 1. \end{aligned} \tag{9}$$

Substituting Eq. (9) into Eq. (8), we obtain

$$X(m) = \sum_{n=0}^{N/2-1} [X_1(n) + (-1)^n X_2(n)]W_{N/2}^{mn/2}, \tag{10}$$

where we use $W_N^{N/2} = -1$ and $W_N^{mn} = W_{N/2}^{mn/2}$. We can also separate Eq. (10) into two parts according to whether m is even or odd:

(a) If m is even, i.e., $m = 2k$, we have

$$X(2k) = \sum_{n=0}^{N/2-1} [X_1(n) + X_2(n)]W_{N/2}^{nk},$$

$$k = m/2 = 0, 1, 2, \ldots, N/2 - 1. \tag{11}$$

(b) If m is odd, i.e., $m = 2k + 1$, we have

$$X(2k + 1) = \sum_{n=0}^{N/2-1} \{[X^1(n) - X_2(n)]W_N^n\}W_{N/2}^{nk},$$

$$k = (m - 1)/2 = 0, 1, 2, \ldots, N/2 - 1. \tag{12}$$

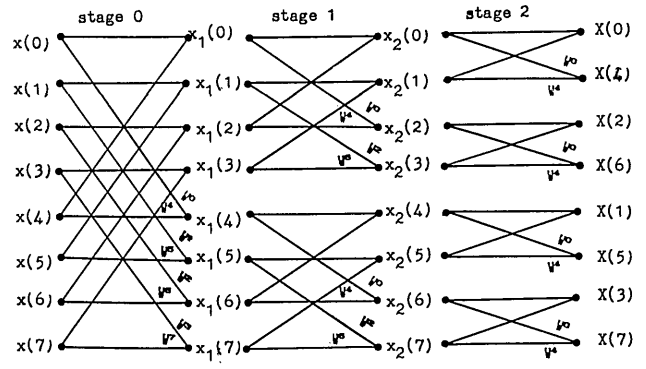

Fig. 5. 1-D butterfly network signal-flow diagram for 1-D FFT's; $N = 8$.

The data flow graph of the 1-D FFT from Eqs. (11) and (12) can constitute a 1-D butterfly interconnection network with the weight factors. Figure 5 is the 1-D butterfly network with size $N = 8$.

Almost all optical information processing is performed in 2-D form. Therefore, studying the 2-D FFT's and building the 2-D optical interconnection networks is a very significant project. For a 2-D general series $X(m, n)$, we have

$$X(u, v) = \sum_{n=0}^{N-1} \sum_{m=0}^{N-1} X(m, n) \exp[-j2\pi(um + vn)/N]. \tag{13}$$

Its FFT can be implemented by performing one 1-D FFT twice. That is, the 2-D signal flow graph can be represented as a set of 1-D transformations on the rows followed by a set of 1-D transformations on the columns.[17,18] As shown in Fig. 6, the size of this network is $N \times N = 4 \times 4$, and the number of link stages is $\log_2^{N\times N} = 2 \log_2^N$, clearly twice that of the 1-D FFT. This interconnection is certainly not suitable for optical interconnections because the number of link stages is too large, and optical interconnections cannot simultaneously implement all the operations within each link stage in parallel. Therefore we want to build the 2-D butterfly interconnection network shown in Fig. 2, in which there are four fan-in and four fan-out lines on each point.

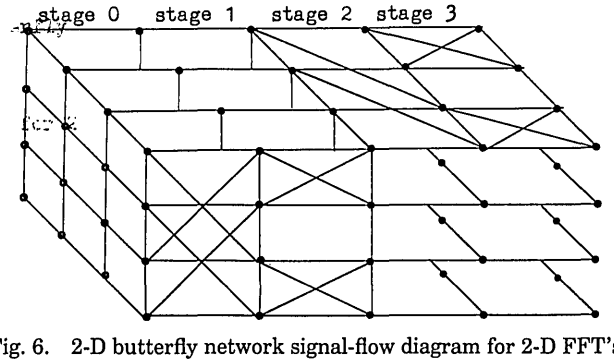

Fig. 6. 2-D butterfly network signal-flow diagram for 2-D FFT's; $N \times N = 4 \times 4$.

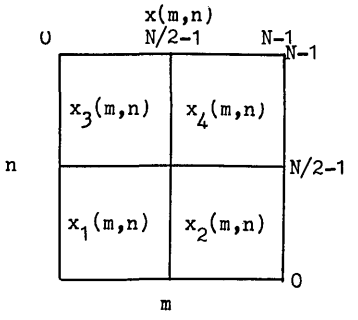

Fig. 7. Separated pattern of a 2-D FFT data array with $N \times N$ points; the four subarrays are represented by $X_1(m, n)$, $X_2(m, n)$, $X_3(m, n)$, and $X_4(m, n)$.

Starting with Eq. (13), we separate the $N \times N$ points of the 2-D FFT into four parts, as shown in Fig. 7, and these four parts are described as

$$\begin{aligned} X_1(m, n) &= X(m, n), \\ X_2(m, n) &= X(m + N/2, n), \\ X_3(m, n) &= X(m, n + N/2), \\ X_4(m, n) &= X(m + n/2, n + N/2), \end{aligned} \tag{14}$$

where $(m, n) = 0, 1, 2, \ldots, N/2 - 1$. Thus Eq. (13) can be represented as

$$\begin{aligned} X(u, v) = \Sigma\Sigma\, &[X_1(m, n) + (-1)^u X_2(m, n) \\ &+ (-1)^v X_3(m, n) + (-1)^{u+v} X_4(m, n)] \\ &\times W_{N/2}^{um} W_{N/2}^{vn}, \end{aligned} \tag{15}$$

where we use $W_N^{N/2} = -1$, $W_N^{um} = W_{N/2}^{um/2}$, and $W_N^{vn} = W_{N/2}^{vn/2}$.

(a) If both u and v are even, i.e., $u = 2i$ and $v = 2j$, then

$$\begin{aligned} X(2i, 2j) = \Sigma\Sigma\, &[X_1(m, n) + X_2(m, n) + X_3(m, n) \\ &+ X_4(m, n)] W_{N/2}^{mi} W_{N/2}^{nj}, \end{aligned} \tag{16}$$

where $i = u/2 = 0, 1, 2, \ldots, N/2 - 1$ and $j = v/2 = 0, 1, 2, \ldots, N/2 - 1$.

(b) If u is even and v is odd, i.e., $u = 2i$ and $v = 2j + 1$, then

$$\begin{aligned} X(2i, 2j + 1) = \Sigma\Sigma\, &\{[X_1(m, n) + X_2(m, n) - X_3(m, n) \\ &- X_4(m, n)] W_N^n\} W_{N/2}^{mi} W_{N/2}^{nj}, \end{aligned} \tag{17}$$

where $i = u/2 = 0, 1, 2, \ldots, N/2 - 1$ and $j = (v - 1)/2 = 0, 1, 2, \ldots, N/2 - 1$.

(c) If u is odd and v is even, i.e., $u = 2i + 1$ and $v = 2j$, then

$$\begin{aligned} X(2i + 1, 2j) = \Sigma\Sigma\, &\{[X_1(m, n) - X_2(m, n) + X_3(m, n) \\ &- X_4(m, n)] W_N^m\} W_{N/2}^{mi} W_{N/2}^{nj}, \end{aligned} \tag{18}$$

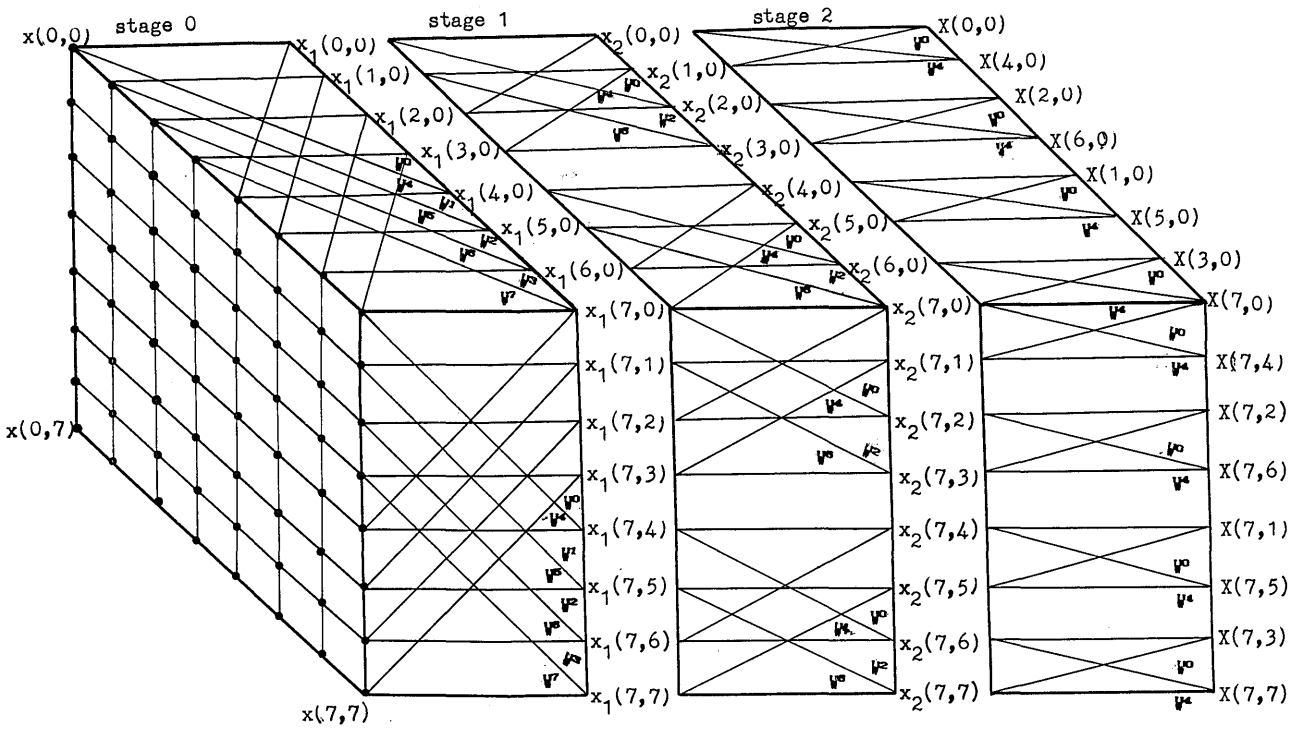

Fig. 8. 2-D butterfly network signal-flow for 2-D FFT's with $N \times N = 8 \times 8$ points.

where $i = (u - 1)/2 = 0, 1, 2, \ldots,$ and $j = v/2 = 0, 1, 2, \ldots, N/2 - 1$.

(d) If both u and v are odd, i.e., $u = 2i + 1$ and $v = 2j + 1$, then

$$X(2i + 2j, + 1) = \Sigma\Sigma \{[X_1(m, n) - X_2(m, n) - X_3(m, n) + X_4(m, n)] W_N^{m+n}\} W_{N/2}^{mi} W_{N/2}^{nj}, \quad (19)$$

where $i = (u - 1)/2 = 0, 1, 2 \ldots,$ and $j = (v - 1)/2 = 0, 1, 2, \ldots, N/2 - 1$.

Therefore the 2-D FFT can be implemented in the 2-D butterfly network signal flow diagram as shown in Fig. 8, in which coefficients W_N^{um} and W_N^{vn} are determined according to Eqs. (16)–(19). This 2-D butterfly flow graph is composed of 8×8 nodes in each node stage. With the 2-D butterfly signal flow diagram defined by Eqs. (16)–(19), we calculate the correlation of the two similar Chinese words that are shown in the right top corner of Fig. 9. As shown, a computer simulation is obtained in which one word pattern is recognized as signal $f(x, y)$ and the other as reference signal $h(x, y)$. Figure 9 is the self-correlation result $g(x', y')$. Therefore we study and build a 2-D system for implementing the FFT-based optical information processing in Section 4.

4. Optical Butterfly Network System Design

With the developments of both optical information processing and computer data processing, hybrid optics and computer information-processing hardware systems have been proposed and researched.[23,24] However, they were based on the combination of optical information-processing systems and electronic computers in which opto-electronic interfaces and analog-to-digital transformations were required. Both the picking up of image samples and the processing of data were performed in series. The success and development of optical interconnection networks, technology, and applications make it possible to study and build the OBNH system for optical information processing on the basis of current optical interconnection technologies.[11–14,16]

The binary phase diffraction gratings (BPDG's) designed to split a single light beam into a specific

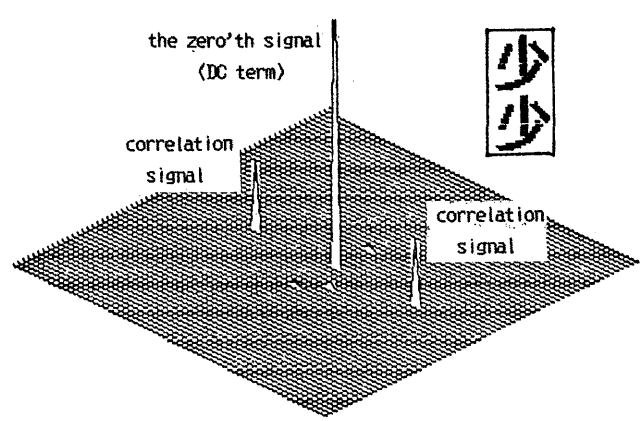

Fig. 9. Result of a computer simulation of the correlation of two similar Chinese words through the 2-D butterfly signal-flow network with $N \times N = 128 \times 128$ points.

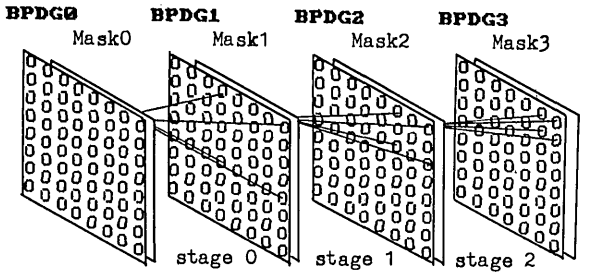

Fig. 10. Arrangement of the 2-D butterfly interconnection with BPDG's and masks.

number of equal intensity diffraction orders have been developed not only to implement free-space optical interconnections with particular constructions[14] but also to perform coherent laser beam additions.[25–27] Because various types of optical information processing based on optical Fourier transformations use coherent light conditions, the OBNH system for performing FFT algorithms can be operated under coherent conditions. The 1-D and 2-D BPDG's have demonstrated their own advantages in implementing manipulator and butterfly networks. These two types of networks are equivalent in topology and similar in construction.[14,21] So it is reasonable to use BPDG's and masks to construct the 1-D and 2-D butterfly interconnection networks. Figure 10 is the arrangement constructed by using BPDG's and masks, in which BPDG's have functions of both beam splitting and coherent addition. A 2-D OBNH system performing 2-D FFT-based optical information processing as shown in Fig. 11 is suggested. The system is composed mainly of two multistage 2-D butterfly networks (each with 8×8 nodes) and a spectrum treating subsystem. In Fig. 11 the butterfly network on the left is used for performing optical FFT's, and the one on the right is used for optical inverse FFT's. If input images or signals are placed on input plane P_1, spatial spectrum patterns can be obtained on spectrum plane P_2. So, in terms of the various requirements for the different types of optical information processing, various frequency-spectrum treating methods can be adopted in the spectrum analysis subsystem. For example, for matched filtering and feature extraction, the filters with various functions can be placed in the spectrum analysis subsystem. For optical pattern recognition and target tracking, the frequency spectra of the reference images or signals can also be inputted directly into the spectrum subsystem, and the required optical images or signals can be obtained on the output plane P_3. Because the output signals throughout the interconnection network system are still discrete points, the output results can be recorded and analyzed by using detectors. Therefore the OBNH system for optical information processing can be used not only to operate numerical calculations but also to perform practical optical experiments. For example, as shown in Fig. 9, because the zeroth-order (dc term) intensity is higher than that of correlation, which seriously

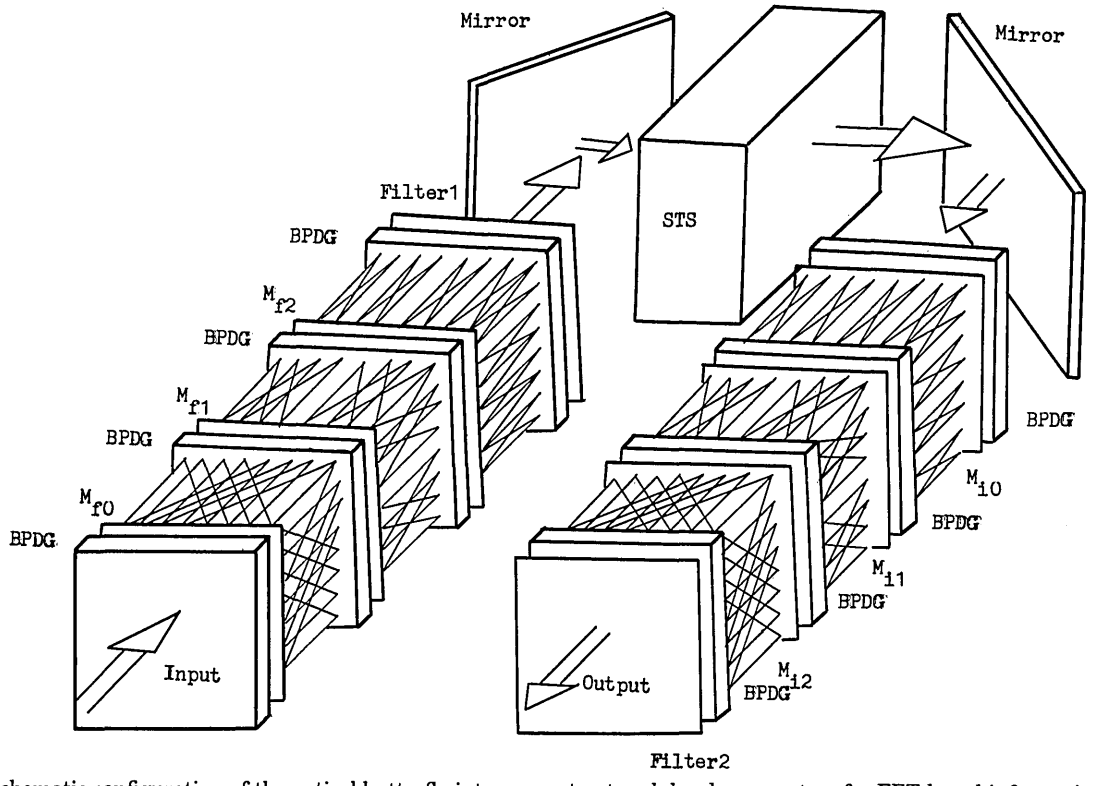

Fig. 11. Schematic configuration of the optical butterfly interconnect network hardware system for FFT-based information processing. Two multistage butterfly networks are used: the one on the left performs the FFT, and the one on the right performs the inverse FFT.

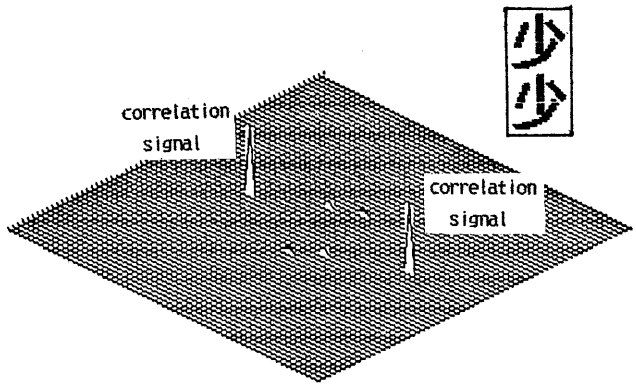

Fig. 12. Result of a computer simulation of the correlation of two similar Chinese words according to the butterfly interconnect network hardware system as shown in Fig. 11, obtained by disconnecting link lines that relay the zeroth-order (dc-term) background information.

influences the observation of correlation signals, enhancing the correlation signal and controlling the zeroth-order background intensities constitutes a problem that optical information-processing experimentation often focuses on. This OBNH system would also be useful in experimentation with pattern recognition and target tracking based on Fourier-transform correlation. However, with the OBNH these problems can be resolved by disconnecting the link lines that relay the zeroth-order background information at the final link stage of the latter network in Fig. 11. Figure 12 is the result of computer simulation with the OBNH system obtained by disconnecting the link lines that relay the zeroth-order background information (shown in Fig. 9). Obviously, there are only correlation signals; there is no the zeroth-order background signal in Fig. 12.

5. Binary Phase Diffraction Grating Features and Mask Patterns

In the OBNH system there are two multistage butterfly networks, one for the FFT's and one for the inverse FFT's. We are considering FFT's of size 8×8 points. Since they are of this size, they require networks containing three link stages, and in each link stage a 2-D BPDG is required. This totals to six BPDG's and correspondingly to six masks for the entire system, as shown in Fig. 11. The BPDG's must serve a double function for laser beams. First, they must split a single beam into two equal (order 0 and ± 1) intensity diffraction orders. Second, they must perform the operation of coherent addition of the zeroth-order and the positive/negative first-order diffraction beams. To achieve these functions, the three BPDG's should all be equivalent in structure. If this condition is met, addition of the zeroth-order beam with the positive/negative first-order beams can be performed in the first-order diffraction angle. The interconnections for various link stages can be designated by controlling the distances (the link

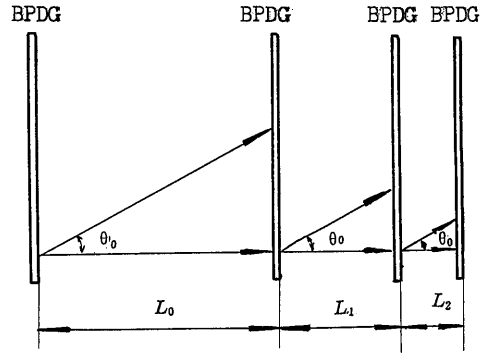

Fig. 13. Relationship of distance L_i between adjacent BPDG's with diffraction angle θ_0.

lengths) L between adjacent BPDG's, as shown in Fig. 13. If, for a link stage i, the distance between two adjacent beams is W_0 and the link length is L_i, then L_i $(i = 0, 1, \ldots, \log_2^M - 1)$ can be defined as

$$L_i = \frac{NW}{2^{i+1} \tan \theta_0}. \tag{20}$$

The transmittance of the grating can be expressed as a superposition of plane waves corresponding to the diffraction orders of the grating:

$$t(X) = \sum_{n=0}^{1} a_n \exp(j\phi_n)\exp(jn\alpha x), \tag{21}$$

where a_n and ϕ_n are the magnitude and phase of the nth beam component and α is proportional to the sine of the angle (θ_0) between the diffraction orders. The gratings are designed such that $a_n \approx a_0$ for the zeroth order and the positive/negative first orders; then

$$\alpha = \alpha_0 \sin \theta_0, \quad \alpha_0 = \text{const.}, \tag{22}$$

$$f(x) = a_0[\exp(j\phi_0)][1 + \exp(jx\alpha_0 \sin \theta_0)]. \tag{23}$$

In Eq. (23) the phase difference between the diffraction orders (orders 1 and 0) is $X \sin \theta_0$. So, according to Figs. 5, 7, and 8, the value of α_0 can be chosen to satisfy the equation $\exp(\alpha_0 \sin \theta_0) = [\exp(-j2\pi/N)]$.

Coherent addition of beams can be accomplished by operating this grating in reverse. This is because the phase of the zeroth order of the grating in the ith node stage is the inverse of the positive/negative first orders of the grating in the $(i + 1)$th node stage.[25–27] The interference patterns of these two beams in the plane of the grating is then given by

$$\begin{aligned} E(x) &= \Sigma \exp(-j\phi_n)\exp(-jn\alpha x) \\ &= \exp(-j\phi_n)[1 + \exp(-jx\alpha_0 \sin \theta_0)]. \end{aligned} \tag{24}$$

The amplitude of the light after it passes through the grating is given by the product of Eqs. (23) and (24) if we consider that $\phi_1 \approx \phi_0$. If the three beams have the same intensity on each node (for a 2-D n-stage

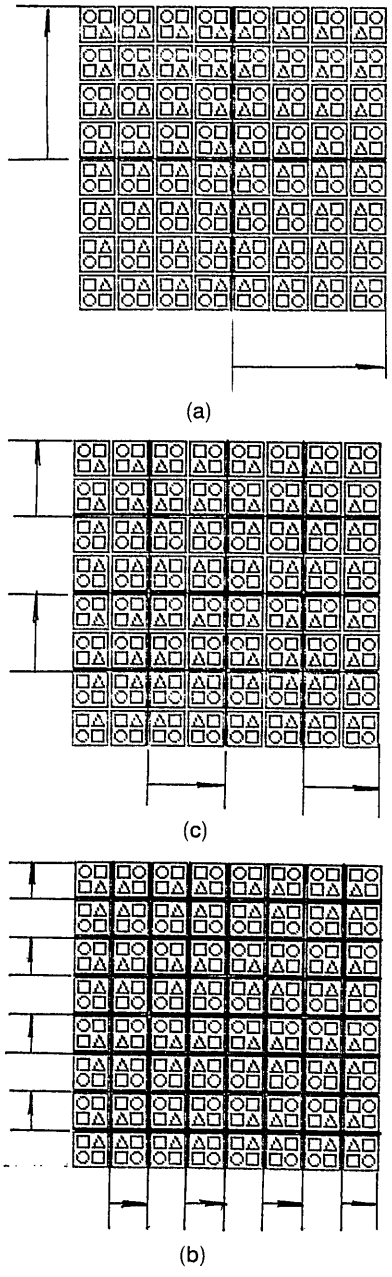

Fig. 14. Patterns of six masks used in the optical butterfly network system shown in Fig. 11: (a) the pattern of M_{f0} and M_{f2}, (b) the pattern of M_{f1} and M_{i1}, and (c) the pattern of M_{f2} and M_{f0}. In all three figures, phase delays per row/column are denoted by circles along, the direction and within the range shown by arrows. Phase increments per row/column are denoted by squares and circles in the areas not indicated by arrows but that occur in the same direction. The phase delays/increments are $\pi/4$ for (a), $\pi/2$ for (b) and $\pi/1$ for (c).

butterfly network), only four out of nine beams are used, which is inefficient. This can be overcome by designing the grating to have only the zeroth order and either the positive-first order or the negative-first order. The patterns of masks M_{f0}, M_{f1}, and M_{f2} in the former butterfly network and M_{i0}, M_{i1}, and M_{i2} in the latter network are used to select the four diffraction beams that constitute the 2-D butterfly network. The patterns of M_{f0}, M_{f1}, and M_{f2} in link stages 0, 1, and 2 are shown in Figs. 14(a), 14(b), and 14(c), respectively, while M_{i0}, M_{i1}, and M_{i2} are the same as M_{f2}, M_{f1}, and M_{f0}, respectively. Within each element (node) in Fig. 14, each circle represents a straightforward link line from the zeroth-order diffraction beam, the two squares represent the butterfly interconnect lines from the first orders along the x and y coordinates, respectively, and each triangle represents the butterfly interconnect line from the first order along the diagonal orientation. In terms of Figs. 5 and 8, the nodes in Fig. 14 whose masks are marked in black frames are required to have phase compensation along both the x and y orientations. The compensated amounts of phases in the different masks are determined by the weighting functions in the butterfly interconnect flow graphs, as shown in Figs. 5 and 8. However, the compensations in the two networks for performing the FFT's and the inverse FFT's are in reverse. That is, if the phases in the former network are compensated, the phases of counterparts in the latter network are delayed proportionately.

6. Summary, Future Work, and Conclusions

For our study of 1-D and 2-D butterfly interconnections and networks in constructions, we first demonstrated the possibility of building the OBNH system for implementing various types of optical information processing, including image processing and signal processing. Then we briefly studied and analyzed key devices such as BPDG's and masks in theory and in structure. With the OBNH system, numerical computations (or analyses) and experimental studies can be performed simultaneously in theory, and the problems such as the zeroth-order (dc term) background intensity can be effectively cancelled, which enhances the correlation signal. This is verified by computer simulation. In theory the OBNH systems based on other transformations such as the Walsh–Hadamard transformation and rapid transformation,[17,18] as well as the unification OBNH systems for optical–digital computing[28] and analog computing and information processing, can also be accomplished. In future research we will study and build an OBNH system, starting with BPDG's masks. Then we will add system spatial light modulators and symmetric self-electro-optic-effect devices to increase the functions of the system in the experiment. Once this is accomplished, the benefits of optical information processing will be within our reach.

The authors thank Hong-Jie Xu for his assistance and support during this work.

References

1. A. VanderLugt, "Signal detection by complex spatial filtering," IEEE Trans. Inf. Theory **IT-10,** 139 (1964).
2. F. T. S. Yu, "Optical information processing," *Optical Signal Processing Fourier Optics* (Wiley/Interscience, New York, 1982).

3. B. Javidi, J. Wang, C. Ruiz, and J. Ruiz, "Nonlinearly transformed baseband filters for optical pattern recognition," Appl. Opt. **30,** 1776–1780 (1991).
4. B. Javidi and J. L. Horner, "Single spatial light modulator joint transform correlator," Appl. Opt. **28,** 1027–1032 (1989).
5. B. Javidi and J. L. Horner, "Multifunction nonlinear signal processor: deconvolution and correlation," Opt. Eng. **28,** 837–846 (1989).
6. J. L. Horner and H. O. Vurtelt, "Two-bit correlation," Appl. Opt. **24,** 2889–2893 (1985).
7. F. T. S. Yu, S. Jutamulia, T. W. Lin, and D. A. Gregory, "Adaptive real-time pattern recognition using liquid crystal," Appl. Opt. **26,** 1370–1372 (1987).
8. F. T. S. Yu and J. E. Ludman, "Micro-computer-based programmable optical correlator for automatic pattern recognition and identification," Opt. Lett. **11,** 395–397 (1986).
9. B. Javidi, "Generalization of the linear matched concept to matched filters," Appl. Opt. **29,** 1215–1224 (1990).
10. K. Fielding and J. L. Horner, "1-*f* binary joint transform correlator," Opt. Eng. **29,** 1081–1087 (1990).
11. T. K. Gaylord, M. Mirsalehi, and C. C. Guest, "Optical digital truth table look-up processing," Opt. Eng. **24,** 48–58 (1985).
12. A. D. McAulay, "Optical crossbar interconnected digital signal processor with basic algorithms," Opt. Eng. **25,** 82–90 (1986).
13. J. Shamir, "Three-dimensional optical interconnection gate array," in *Selected Papers on Optical Computing,* H. J. Caulfield and G. Gheen, eds., Proc. Soc. Photo-Opt. Instrum. Eng. **1142,** 414 (1989).
14. T. J. Cloonan and M. J. Herron, "Optical implementation and performance of one-dimensional and two-dimensional trimmed inverse augmented data manipulator networks for multiprocessor computer systems," Opt. Eng. **28,** 305–314 (1989).
15. B. Javidi, "Comparison of binary joint transform image correlators and phase-only matched filter correlators," Opt. Eng. **28,** 267–272 (1989).
16. M. E. Prise, N. C. Craft, M. M. Down, R. E. LaMarche, L. A. D'Asaro, L. M. F. Chirovsky, and M. J. Murdocca, "Optical digital processor using arrays of symmetric self-electronic effect devices," Appl. Opt. **30,** 2289–2296 (1991).
17. E. O. Brigha, *The Fast Fourier Transform and Its Applications* (Prentice-Hall, Englewood Cliffs, N.J., 1988), pp. 131–266.
18. D. F. Elliott and K. E. Rao, *Fast Transforms: Algorithms, Analyses, and Applications* (Academic, New York, 1982), pp. 54–411.
19. M. J. Alallah, "Multidimensional arrays of processors," IEEE Trans. Comput. **37,** 1306–1309 (1988).
20. C. L. Wu and T. Y. Feng, "On a class of multistage interconnection networks," IEEE Trans. Comput. **C-29,** 694-702 (1980).
21. T. J. Cloonan, "Topological equivalence of optical crossover networks and modified data manipulator networks," Appl. Opt. **28,** 2494–2498 (1989).
22. T. J. Cloonan and F. B. McCormick, "Photonic switching applications of 2-D and 3-D crossover networks based on 2-input, 2-output switching nodes," Appl. Opt. **30,** 2309–2332 (1991).
23. D. Casasent and W. Sterling, "A hybrid optical/digital processor: hardware and applications," IEEE Trans. Comput. **C-24,** 348–357 (1975).
24. H. Stark, "An optical–digital computer for parallel processing of images," IEEE Trans. Comput. **C-24,** 340–345 (1975).
25. J. R. Leger, G. J. Swanson, and W. B. Veldkamp, "Coherent laser addition using binary phase gratings," Appl. Opt. **26,** 4391–4399 (1988).
26. W. B. Veldkamp, J. R. Leger, and G. J. Swanson, "Coherent beam addition of GaAlAs by binary phase gratings," Appl. Phys. Lett. **11,** 303–305 (1986).
27. J. R. Leger, G. J. Swanson, and W. B. Veldkamp, "Coherent beam addition of GaAlAs lasers by binary phase gratings," Appl. Phys. Lett. **11,** 888 (1986).
28. D. G. Sun, Q. Xiang, N. X. Wang, and Z. H. Weng, "Butterfly interconnection implementation for an *n*-bit parallel full adder/subtractor," Opt. Eng. **31,** 1568–1575 (1992).